Check for updates

S100A8 and S100A9 are elevated in chronically threatened ischemic limb muscle and induce ischemic mitochondrial pathology in mice

Zachary R. Salyers, MS,[a] Vinicius Mariani, MS,[a] Nicholas Balestrieri, MS,[a] Ravi A. Kumar, MS,[a] Nicholas A. Vugman,[a] Trace Thome, MS,[a] Katelyn R. Villani, MS,[a] Scott A. Berceli, MD, PhD,[b,e] Salvatore T. Scali, MD,[b,e] Georgios Vasilakos, PhD,[a] *and* Terence E. Ryan, PhD,[a,c,d] *Gainesville, FL*

ABSTRACT

Objective: The objective of the present study was to determine whether elevated levels of S100A8 and S100A9 (S100A8/A9) alarmins contribute to ischemic limb pathology.

Methods: Gastrocnemius muscle was collected from control patients without peripheral arterial disease (PAD; n = 14) and patients with chronic limb threatening limb ischemia (CLTI; n = 14). Mitochondrial function was assessed in permeabilized muscle fibers, and RNA and protein analyses were used to quantify the S100A8/A9 levels. Additionally, a mouse model of hindlimb ischemia with and without exogenous delivery of S100A8/A9 was used.

Results: Compared with the non-PAD control muscles, CLTI muscles displayed significant increases in the abundance of S100A8 and S100A9 at both mRNA and protein levels ($P < .01$). The CLTI muscles also displayed significant impairment in mitochondrial oxidative phosphorylation and increased mitochondrial hydrogen peroxide production compared with the non-PAD controls. The S100A8/A9 levels correlated significantly with the degree of muscle mitochondrial dysfunction ($P < .05$ for all). C57BL6J mice treated with recombinant S100A8/A9 displayed impaired perfusion recovery and muscle mitochondrial impairment compared with the placebo-treated mice after hindlimb ischemia surgery. These mitochondrial deficits observed after S100A8/A9 treatment were confirmed in the muscle cell culture system under normoxic conditions.

Conclusions: The S100A8/A9 levels were increased in CLTI limb muscle specimens compared with the non-PAD control muscle specimens, and the level of accumulation was associated with muscle mitochondrial impairment. Elevated S100A8/A9 levels in mice subjected to hindlimb ischemia impaired perfusion recovery and mitochondrial function. Together, these findings suggest that the inflammatory mediators S100A8/A9 might be directly involved in ischemic limb pathology. (JVS—Vascular Science 2022;3:232-45.)

Clinical Relevance: Despite improvements in the surgical management of chronic limb threatening limb ischemia (CLTI), the rates of major adverse limb events have remained high. Skeletal muscle has emerged as a strong predictor of outcomes in peripheral arterial disease (PAD)/CLTI; however, a complete understanding of muscle pathology in CLTI is lacking. This study identified elevated S100A8 and S100A9 alarmin proteins as a characteristic of CLTI muscle specimens and that the S100A8/A9 levels are associated with the degree of mitochondrial impairment in patient limb muscle specimens. Using a mouse model of PAD, treatment with S100A8/A9 exacerbated ischemic limb pathology, including impaired limb perfusion recovery and muscle mitochondrial impairment. Taken together, these findings connect the inflammatory milieu in the CLTI limb to exacerbated limb muscle outcomes via mitochondrial alterations.

Keywords: Inflammation; Mitochondria; Peripheral artery disease; Vascular disease

Peripheral arterial disease (PAD) is caused by atherosclerotic occlusion of peripheral blood vessels, resulting in limb ischemia. Chronic limb threatening ischemia (CLTI) is the most severe presentation of PAD and includes ischemic rest pain and often coincides with tissue ulcers or nonhealing wounds. CLTI patients often have numerous comorbid conditions that contribute to worse health outcomes, including a high risk of limb amputation or death. Systemic inflammation is common in patients with PAD or CLTI[1–5]; however, little is known

From the Department of Applied Physiology and Kinesiology,[a] Department of Surgery,[b] Center for Exercise Science,[c] and Myology Institute,[d] University of Florida; and the Malcom Randall Veterans Affairs Medical Center.[e]

The present study was supported by the National Institutes of Health (grant R01HL149704 to T.E.R.) and the American Heart Association (grant 18CDA34110044 to T.E.R.).

Author conflict of interest: none.

Correspondence: Terence E. Ryan, PhD, Department of Applied Physiology and Kinesiology, University of Florida, 1864 Stadium Rd, Gainesville, FL 32611 (e-mail: ryant@ufl.edu).

The editors and reviewers of this article have no relevant financial relationships to disclose per the JVS-Vascular Science policy that requires reviewers to decline review of any manuscript for which they may have a conflict of interest.

2666-3503

Copyright © 2022 by the Society for Vascular Surgery. Published by Elsevier Inc. This is an open access article under the CC BY-NC-ND license (http://creativecommons.org/licenses/by-nc-nd/4.0/).

https://doi.org/10.1016/j.jvssci.2022.03.003

about the underlying biology by which this inflammatory state might contribute to ischemic limb pathology.

Recent studies have implicated S100A8 and S100A9 (S100A8/A9), proinflammatory calcium binding proteins from the S100 family known as alarmins, as regulators of ischemic pathology in the myocardium.[6–10] S100A8/A9 are expressed abundantly in immune cells (neutrophils and macrophages) that infiltrate tissues after ischemic events, environmental triggers, and/or cellular damage and can be released at these local sites from these phagocytes.[11] The S100 family members S100A8 and S100A9 are the best studied and are found primarily as heterodimers in vivo (excellent reviews on S100 proteins have been provided by Sreejit et al[12,13]). Within cells, these alarmins participate in cytoskeletal rearrangements and alter the metabolism but are actively released from immune cells during inflammation to contribute to leukocyte recruitment and subsequent cytokine secretion.[13,14] S100A8/A9 are also known ligands for toll-like receptor 4 and the receptor for advanced glycation end products, which have been implicated in the pathologic effects of these alarmins.[6,10,15,16] In patients, the plasma levels of S100A8/A9 correlate with circulating neutrophil counts and have been associated with cardiovascular disease risk.[17] Mechanistically, S100A8/A9 were recently shown to cause cardiomyocyte mitochondrial dysfunction (inhibition of complex I of the electron transport system) and to increase cell death after myocardial infarction in mice.[18] Another group recently reported that treatment with a selective S100A9 blocker, ABR-238901, significantly improved cardiac function in mice after myocardial infarction.[19]

Information regarding the relevance of these alarmins to PAD has begun to emerge in the literature. A recent study from Spain reported that elevated S100A9 levels in extracellular vesicles obtained from serum distinguished patients with intermittent claudication from controls and patients with CLTI from those with intermittent claudication.[20] Furthermore, they reported that S100A9 levels had prognostic value in relation to major adverse cardiovascular events and amputation outcomes.[20] Of relevance to human patients with PAD, a recent study of diabetic mice demonstrated that pharmacologic blockage of S100A8/A9 reduced atherogenesis.[21] In the murine hindlimb ischemia model, Ganta et al[22] demonstrated that VEGFR1 (vascular endothelial growth factor receptor 1) inhibition by the antiangiogenic isoform $VEGF_{165}b$ in macrophages resulted in S100A8/A9-mediated calcium influx, inducing an M1-like phenotype and impairing ischemic tissue regeneration. Combined with the abundance of data from myocardial ischemia, these findings suggest that S100A8/A9 might play a significant role in PAD pathobiology. Thus, we hypothesized that elevated S100A8/A9 levels would contribute to exacerbated ischemic limb pathology. Therefore, we first assessed the S100A8/A9 levels in CLTI and non-PAD limb muscle specimens. Next, we treated C57BL6J mice with exogenous S100A8/A9 to determine whether increasing the levels of these alarmins would exacerbate ischemic limb pathology.

ARTICLE HIGHLIGHTS

- **Type of Research:** A study using a mouse model of peripheral arterial disease and human study of chronic limb threatening ischemia (CLTI) muscle specimens
- **Key Findings:** S100A8 and S100A9 (S100A8/A9) were elevated in the CLTI patient limb muscles (n = 14), and the elevation was associated with mitochondrial impairment. In the mouse model, treatment with S100A8/A9 decreased limb perfusion recovery and caused muscle mitochondrial dysfunction after femoral artery ligation.
- **Take Home Message:** The results of our study indicate that S100A8/A9, a regulator of inflammatory and immune responses, might contribute to ischemic limb pathology in peripheral arterial disease and CLTI.

METHODS

Human study populations and specimen collection.

Gastrocnemius muscle specimens were collected from 14 older adult non-PAD controls and 14 CLTI patients undergoing limb amputation (5 above the knee and 5 below the knee) or surgical intervention (angioplasty for 2 and bypass for 2). Of the CLTI amputation specimens, four were collected from patients with nonhealing ulcers or gangrene. Seven patients had undergone previous surgical interventions (three angioplasty; four bypass), and one sample was obtained from a CLTI patient with nonreconstructable disease. The specimen was collected from the largest circumference of the calf muscle from the medial head of the gastrocnemius muscle. The muscle specimens were collected within the confines of the operating room for the CLTI patients or via percutaneous muscle biopsy using previously described sterile procedures.[23,24] A portion of the muscle was quickly trimmed of fat and connective tissue and snap frozen in liquid nitrogen for analysis. Another portion of the fresh muscle specimen was processed immediately for mitochondrial function assessment as described in detail in the next sections and in previous studies.[24] Owing to the limited specimen size with percutaneous biopsies, histologic analysis of the muscle fiber number or size was

not possible in the present study. The institutional review board at the University of Florida and Malcom Randall Veterans Affairs Medical Center approved the present study (protocol nos. IRB201802025 and IRB201801553). All study procedures were performed in accordance with the Declaration of Helsinki. The participants were fully informed about the research and provided written informed consent.

Tandem mass tag-labeled proteomics analysis of human skeletal muscle. A portion of the snap frozen muscle specimen was used for isobaric tandem mass tag-labeled proteomic analysis. We described the tissue processing, mass spectrometry analysis, and bioinformatics for these samples in our previous study.[25] Protein abundance for S100A8 and S100A9 from these proteomics analyses was converted to the Log2 space for group comparisons. For each comparison, protein abundance was analyzed for the group average, standard deviation, two-tailed Student's *t* test (equal variance), and a Benjamini-Hochberg false discovery rate-corrected adjusted *P* value. All raw proteomics data are available online using accession number PXD021849 (Proteome Xchange Consortium; available at: http://www.proteomexchange.org/) or JPST000852 (Japan Proteome Standard Repository; available at: https://repository.jpostdb.org/).

mRNA analysis of human skeletal muscle. A portion of snap frozen muscle was used for RNA isolation using Trizol reagent to homogenize the specimen and the Direct-zol RNA miniprep kit (model no. R2072; Zymo Research, Irvine, CA) in accordance with the manufacturer's instructions. Following RNA isolation, cDNA was synthesized using 200 ng of RNA with the qScript cDNA synthesis kit (model no. 95047-500; Quantabio, Beverly, MA). Real-time polymerase chain reaction was performed using QuantStudio 3 (Applied Biosystems, Waltham, MA) with the TaqMan fast advanced master mix (Applied Biosystems) and the following TaqMan probes: Hs00374264_g1 (S100A8), Hs00610058_m1 (S100A9), and Hs03003631_g1 (18S). Gene expression was normalized to the internal loading control 18S, and relative changes in the mRNA levels were quantified using the $^{\Delta\Delta}$CT method.

Preparation of permeabilized human muscle fibers. A portion of the muscle biopsy specimen was dissected and immediately placed in ice-cold buffer X (50 mM K-MES, 7.23 mM K_2EGTA, 2.77 mM CaK_2EGTA, 20 mM imidazole, 20 mM taurine, 5.7 mM adenosine triphosphate [ATP], 14.3 mM phosphocreatine, and 6.56 mM $MgCl_2$-$6H_2O$; pH 7.1) for preparation of permeabilized fiber bundles, as previously described by our group.[23,26] Before loading the fiber bundles for experimentation, they were gently blotted on a Kimwipe (Kimberly-Clark Professional Kimtech Science; Thermo Fisher Scientific, Waltham, MA) for exactly 5 seconds, and a wet weight was obtained using a Mettler Toledo MX5 microbalance (Mettler Toledo, Columbus, OH).

Mitochondrial respiration measurements in human muscle fibers. High-resolution oxygen consumption measurements were conducted at 37°C in buffer Z (105 mmol/L K-MES, 30 mmol/L KCl, 1 mmol/L EGTA, 10 mmol/L K_2HPO_4, 5 mmol/L Mg Cl_26H_2O, 0.5 mg/mL bovine serum albumin [BSA]; pH 7.1), supplemented with creatine monohydrate (5 mM), using an O2K Oxygraph (Oroboros Instruments, Innsbruck, Austria).[27] To assess mitochondrial function under physiologically relevant conditions, we used a novel creatine kinase (CK) clamp system to set the level of cellular energy demand to which the fiber bundles were exposed.[28,29] First, the bundles were energized with either carbohydrate (5 mM pyruvate and 2.5 mM malate) or fatty acid (0.2 mM octanoylcarnitine and 2.5 mM malate), and measurements of state 2 oxygen consumption were collected. Next, the CK clamp was added, which included 20 U/mL of creatine kinase, 5 mM ATP, and 1 mM phosphocreatine (PCr) to mimic near maximal exercise conditions. PCr was subsequently added in a stepwise fashion to reduce the cellular energy demand to resting conditions. The slope of the relationship between the cellular energy demand (ΔG_{ATP}) and oxygen consumption (JO_2) was calculated. The rate of respiration was expressed as pmol/s/mg fiber wet weight. All respiration measurements were conducted at 37°C and a working range [O_2] of ~350 to 200 μM.

Mitochondrial hydrogen peroxide emission. Mitochondrial hydrogen peroxide (H_2O_2) emission was measured in the bundles fluorometrically at 37°C via the Amplex UltraRed (10 μM)/horseradish peroxidase (3 U/mL) detection system (Thermo Fisher Scientific; excitation/emission 565/600) using a Horiba Quantamaster 400 (Horiba, Kyoto, Japan), as previously described.[27,30] This analysis was performed using the identical substrate conditions described in the previous sections. The fluorescence units were converted to pmols of H_2O_2 using a standard curve.

Mice. C57BL/6J male mice (stock no. 000664) were obtained from The Jackson Laboratory (Bar Harbor, ME) and used at 12 weeks of age (n = 20 total). All the mice were housed in a temperature-controlled (22°C) and light-controlled (12-hour light/12-hour dark) room and fed a standard chow diet with free access to food and water. All animal experiments adhered to the Guide for the Care and Use of Laboratory Animals from the Institute for Laboratory Animal Research (National Research Council,

Washington, DC, 1996 and any updates). The institutional animal care and use committee of the University of Florida approved all the procedures.

Hindlimb ischemia surgery. Unilateral hindlimb ischemia was induced by anesthetizing the mice with an intraperitoneal injection of ketamine (90 mg/kg) and xylazine (10 mg/kg) and surgically placing silk ligatures on the femoral artery from its origin just distal the inguinal ligament and immediately distal to the proximal caudal femoral artery. Superficial limb necrosis was not observed in any of the mice.[31] At 7 days after induction of hindlimb ischemia, the mice were anesthetized with ketamine and xylazine for muscle tissue procurement and the experiments as described in the next sections.

Laser Doppler limb perfusion measurements. Limb perfusion was measured using a laser Doppler flowmeter (moorVMS-LDF; Moor Instruments, Wilmington, DE) before surgery, immediately after surgery, and just before sacrifice (7 days after surgery) under ketamine and xylazine anesthesia. In brief, the hindlimbs were shaved to remove the hair, and the laser Doppler probe was carefully placed against the skin of the lateral head of the gastrocnemius muscle and the bottom of the paw. Data were collected continuously for 60 seconds, and the average perfusion rate was calculated. Perfusion recovery in the ischemic limbs was calculated as a percentage of the nonischemic control limb, as previously described.[32,33]

Skeletal muscle morphology. Skeletal muscle morphology was assessed using standard light microscopy. Transverse sections, 10-μm thick, from the tibialis anterior muscle were cut using a cryotome (model no. CM3050S; Leica Biosystems, Baden-Wurttemberg, Germany) and collected on slides for staining. For morphologic analyses, the standard methods for hematoxylin and eosin histologic staining were used, and images were obtained at 20× magnification using automated image capture and/or tiling to image the entire muscle section using an Evos FL2 Auto microscope (Thermo Fisher Scientific). All image analyses were conducted by a blinded investigator using ImageJ (National Institutes of Health, Bethesda, MD). Injured or regenerating myofibers were quantified by manually counting the fibers with centralized nuclei from the entire section of the muscle (imaged and tiled together).

Immunofluorescence microscopy. The skeletal myofiber cross-sectional area and capillary density were assessed in mouse skeletal muscles using immunofluorescence microscopy, as previously described.[34,35] We cut 10-μm-thick transverse sections from the tibialis anterior muscle. The sections were fixed with 4% paraformaldehyde, subsequently blocked for 1 hour at room temperature with phosphate-buffered saline (PBS) supplemented with 5% goat serum and 1% BSA, and incubated overnight at 4°C with a primary antibody for laminin (1:100; catalog no. L9393; Sigma-Aldrich, St Louis, MO) to label the myofibers membrane. Following washes with PBS, the sections were incubated with Alexa-Fluor secondary antibodies (1:250; Thermo Scientific Fisher) and Dylight594-conjugated *Griffonia simplicifolia* I isolectin B4 (DL-1207; Vector Laboratories, Burlingame, CA) to label endothelial cells (ie, capillaries). Coverslips were mounted with Vectashield HardSet mounting medium containing DAPI (4′,6-diamidino-2-phenylindole; H-1500; Vector Laboratories). Images were obtained at 20× magnification using an Evos FL2 Auto microscope (Thermo Fisher Scientific). All image analyses were performed using MuscleJ, an automated image analysis program in Fiji.[36] The total capillary counts were collected from the tiled images of the entire tibialis anterior muscle of each mouse.

Assessment of muscle contractile function. Muscle contractile function was assessed ex vivo in the extensor digitorum longus muscle, as previously described.[33–35,37,38] We measured the isometric forces at stimulation frequencies of 1, 20, 40, 60, 100, and 150 Hz using a biphasic high-power stimulator (701C; Aurora Scientific, Aurora, ON, Canada) delivered with current of 600 mA, pulse duration of 0.25 ms, and train duration of 500 ms, with each stimulation train separated by 1-minute intervals of rest. The isometric forces were normalized by the cross-sectional area, which was estimated by measuring the muscle weight and length at the optimal muscle length. The muscle weight was divided by the length multiplied by 1.06 g/cm^3, the density of mammalian skeletal muscle.[39]

Mouse muscle mitochondrial isolation and respiratory function. Hindlimb muscle mitochondrial respiratory function was tested using the gastrocnemius muscle in the hindlimb and was isolated as previously reported.[22,24] Using the CK clamp system described, respiratory function was assessed at 37°C in buffer Z (in mmol/L) supplemented with creatine monohydrate (5 mM), using the O2K Oxygraph (Oroboros Instruments). Isolated mitochondria were energized with pyruvate and malate (5 mM and 2.5 mM, respectively) to obtain state 2 respiration, followed by addition of the CK clamp and the addition of PCr to titrate the energy demand from a mimicked high exercise level to resting levels. The slope of the relationship between the cellular energy demand (ΔG_{ATP}) and oxygen consumption (JO_2) was calculated. The rate of respiration was expressed as pmol/s/mg of mitochondria. All respiration measurements were conducted at 37°C and a working range [O_2] of ~200 μM. H_2O_2 production was assessed using pyruvate and malate and identical energy demands as performed using

the O2K Oxygraph (Oroboros Instruments) via the Amplex UltraRed (10 μM)/horseradish peroxidase (3 U/mL) detection system (Thermo Fisher Scientific), as previously described.[21,24]

Muscle cell culture. C2C12 muscle cells were obtained from American Type Culture Collection (myoblast cell line, CRL-1772) and cultured in *Dulbecco's modified Eagle medium* supplemented with 10% fetal bovine serum and 1% penicillin/streptomycin in standard conditions (37°C; 5% carbon dioxide). Myoblast differentiation was initiated by serum withdrawal using Dulbecco's modified Eagle medium supplemented with 2% heat-inactivated horse serum and 1% penicillin/streptomycin. All culture experiments were performed in three biologically independent lots.

Myotube atrophy. Myoblasts were differentiated for 7 days before treatment with recombinant S100A8/A9 (rS100A8/A9; 1000 ng/mL) or placebo (PBS supplemented with 0.1% BSA). After 24 hours of treatment with rS100A8/A9 or placebo, the cells were washed with PBS, fixed with 100% methanol for 10 minutes, left to air dry for 10 minutes, and incubated with primary antibody against sarcomeric myosin (MYH1E antibody was deposited to the Developmental Studies Hybridoma Bank by Fischman DA; DSHB Hybridoma Product) at 1:25 in blocking solution for 1 hour at 37°C. The cells were then washed three times in PBS, followed by incubation with 1:250 secondary antibody (AlexaFluor594, mouse IgG2b; Thermo Fisher Scientific) for 1 hour at 37°C. The myotubes were then washed three times in PBS and imaged using automated capture routines with an Evos FL Auto 2 inverted fluorescent microscope (Thermo Fisher Scientific). Each well was imaged using automation to cover 60% of the well starting from the center. The myotube area (MYH1E antibody-positive area) was analyzed using custom written routines in CellProfiler (Broad Institute of MIT and Harvard, Cambridge, MA). All processing procedures were performed uniformly over the entire set of images using batch processing modes to remove any human input.

Myotube mitochondrial function. C2C12 myoblasts were differentiated for 7 days before treatment with rS100A8/A9 (1000 ng/mL) or placebo (PBS supplemented with 0.1% BSA) for 24 hours. Following treatment, the myotubes were washed one time with PBS, trypsinized and collected, and centrifuged at 800*g* for 5 minutes. The pelleted cells were then resuspended in buffer Z supplemented with 5 mM creatine. Respiratory function was assessed via the O2k Oxygraph (Oroboros Instruments) at 37°C and a working range [O_2] of ~350 to 200 μM. First, intact cell respiration was acquired, followed by the addition of digitonin (10 μg/mL) to permeabilize the cells. Pyruvate (5 mM) and malate (2.5 mM) were added to induce state 2 respiration, followed by implementation of the CK clamp and sequential titrations of PCr to determine the respiratory function at each energy demand imposed (ΔG_{ATP} , 54.12-63.8 kJ/mol), and mitochondrial *oxidative phosphorylation* conductance was determined as the slope of the JO_2 vs ΔG_{ATP} relationship. As described, H_2O_2 was also assessed in myotubes using the Amplex UltraRed (10 μM)/horseradish peroxidase (3 U/mL) detection system (Thermo Fisher Scientific).

Statistical analysis. The data are presented as the mean ± standard deviation. The normality of all the data was assessed using the Shapiro-Wilk test. Data that were not normally distributed were analyzed using a Kruskal-Wallis test. Comparisons across the two groups were performed using one-way analysis of variance with Tukey's post hoc multiple comparisons when pairwise comparisons were appropriate or a two-tailed Student's *t* test otherwise. A χ^2 test was used analyze the differences in population proportions for the relevant clinical characteristics. All statistical analyses were performed using Prism, version 8.0 (GraphPad, San Diego, CA), or Vassar Stats (available at: http://vassarstats.net). In all cases, $P < .05$ was considered statistically significant.

RESULTS

S100A8 and S100A9 are elevated in CLTI limb muscle specimens. In the present study, limb muscle specimens were collected from non-PAD control participants and CLTI patients undergoing limb amputation or surgical intervention. The physical and clinical characteristics of the study participants are listed in the Table. The CLTI and non-PAD control groups were relatively well-matched for age. However, the control group had fewer comorbid conditions and less medication usage. The CLTI patient comorbidities included hypertension (100%), hyperlipidemia (100%), diabetes mellitus (64%), coronary artery disease (64%), chronic obstructive pulmonary disease (21%), and renal disease (21%). Most (79%) of the CLTI patients were either former or active smokers. In contrast, only 36% of the non-PAD control group were either former or active smokers.

We previously reported the results of a proteomic analysis of CLTI limb muscle (accession no. PXD021849 [Proteome Xchange Consortium]; or accession no. JPST000852 [Japan Proteome Standard Repository]).[25] Although not the focus of our previous study, the protein abundance of S100A8 and S100A9 was significantly higher in the CLTI muscle than in the non-PAD control muscle (Fig 1, *A*). These results were further confirmed at the mRNA level using real-time polymerase chain reaction. The CLTI limb muscle displayed greater mRNA levels of both S100A8 and S100A9 compared with the non-PAD control muscles (Fig 1, *B*). The patients with the highest protein or mRNA abundance of S100A8/A9 had all had a diagnosis of Rutherford class 5 and 6. In contrast, some patients with Rutherford class 4 had displayed expression levels

Table. Physical and clinical characteristics

Characteristic	Control (n = 14)	CLTI (n = 14)	*P* value
Age, years	71.9 ± 6.3	68.5 ± 7.2	.299[a]
Female sex	4 (29)	1 (7)	**.044**
Overweight/obese (BMI ≥25 kg/m^2)	9 (64)	9 (64)	1.000
ABI	1.09 ± 0.11	0.53 ± 0.25[b]	**<.001**[a]
Rutherford classification			
0	14 (100)	0 (0)	**<.001**
4	0 (0)	6 (43)	.624
5	0 (0)	6 (40)	.646
6	0 (0)	2 (14)	.454
Medical history			
Diabetes mellitus, type 1 or 2	6 (43)	9 (64)	.108
Hypertension	8 (57)	14 (100)	**.010**
Hyperlipidemia	6 (43)	14 (100)	**.006**
Coronary artery disease	2 (14)	9 (64)	**.004**
Renal disease	0 (0)	3 (21)	.183
COPD	1 (7)	3 (21)	.283
Tobacco use	5 (36)	11 (79)	**.001**
Former smoker	3 (21)	8 (57)	**.006**
Current smoker	2 (14)	3 (21)	.335
Medication			
Aspirin	5 (36)	10 (71)	**.007**
Statin	5 (36)	14 (100)	**<.001**
ACE inhibitor	5 (50)	6 (60)	.784
Cilostazol	0 (0)	6 (43)	**<.001**

ABI, Ankle brachial index; *ACE,* angiotensin-converting enzyme; *BMI,* body mass index; *CLTI,* chronic limb threatening ischemia; *COPD,* chronic obstructive pulmonary disease.
Data presented as mean ± standard deviation or number (%).
Boldface *P* values represent statistical significance.
[a] *t* Test (two-tailed); all other *P* values computed using a χ^2 test (performed to determine differences in population proportions).
[b] Four patients with CLTI had noncompressible vessels, precluding ABI measurement.

near those of the control group. A representative image of hematoxylin and eosin–stained muscle sections confirmed the presence of immune and inflammatory cell infiltrates and evidence of myopathy, including fibers with centralized nuclei, an irregular fiber shape, and necrotic myofibers (Fig 1, *C*).

S100A8 and S100A9 protein levels correlate with mitochondrial impairment in CLTI. Consistent with our previous reports,[24,25] we found that CLTI patients displayed significant impairment in mitochondrial oxidative phosphorylation. In the present study, we used a novel CK clamp system to test the mitochondrial oxidative phosphorylation function across a range of physiologic relevant energy demands to mimic a stress test that ranges from rest to exercise. Whether energized with saturating concentrations of carbohydrates (pyruvate and malate) or fatty acids (octanoylcarnitine and malate), the CLTI muscle bundles displayed significantly lower rates of oxygen consumption compared with the non-PAD control muscle bundles (Fig 2, *A* and *C*). Quantification of the slope of these graphs provided an index of oxidative phosphorylation function (termed conductance), which was significantly lower in the CLTI muscle with both carbohydrates (Fig 2, *B*) and fatty acids (Fig 2, *D*). Correlational analyses revealed a significant inverse relationship between the protein abundance of S100A8 or S100A9 and oxidative phosphorylation function (Fig 2, *E*), a finding consistent with that from a previous study reporting that these alarmins impair mitochondrial function in the heart muscle.[18]

Next, we used the same mitochondrial stress testing procedure to examine mitochondrial H_2O_2 production, a well-known reactive oxygen species. Using the Amplex UltraRed fluorescent dye, the CLTI muscle bundles displayed significantly greater levels of H_2O_2 production compared with the non-PAD control muscle bundles for both carbohydrate (Fig 3, *A*) and fatty acid (Fig 3, *B*) substrates. Correlational analyses demonstrated a significant positive correlation between the protein abundance of S100A8 or S100A9 and the level of H_2O_2 production at a resting energy demand (ΔG_{ATP}, 63.90 kJ/mol) regardless of the substrate (Fig 3, *C*). Taken together, these findings suggest that the level of S100A8 and/or S100A9 in the ischemic limb could be a contributing factor to the degree of mitochondrial pathology in CLTI.

Treatment with S100A8/A9 impairs perfusion recovery by not muscle contraction in C57BL6J mice. To examine a potential causal relationship between ischemic limb pathology and S100A8/A9 levels, we used the widely accepted hindlimb ischemia model of PAD in mice. C57BL6J mice received an intraperitoneal injection of recombinant S100A8/A9 (50 μg/kg body weight) or placebo (0.1% BSA in sterile saline) the day before surgery and subsequently every other day until sacrifice (Fig 4, *A*). The mice treated with rS100A8/A9 showed significantly impaired perfusion recovery in the gastrocnemius muscle ($P < .05$) and a nonsignificant decrease in paw perfusion ($P = .09$; Fig 4, *B*). The total capillary count in the nonischemic or ischemic tibialis anterior muscle was not different between groups (Fig 4, *C*). Histologic analysis of the tibialis anterior muscle showed a similar degree of muscle injury and regeneration, evidenced by equal numbers of myofibers with centralized nuclei and myofiber sizes (Fig 4, *D-F*). In line with the histologic evidence, the force-producing capacity of the muscle was not altered by rS100A8/A9 treatment in either the control or ischemic extensor digitorum longus muscles (Fig 4, *G*).

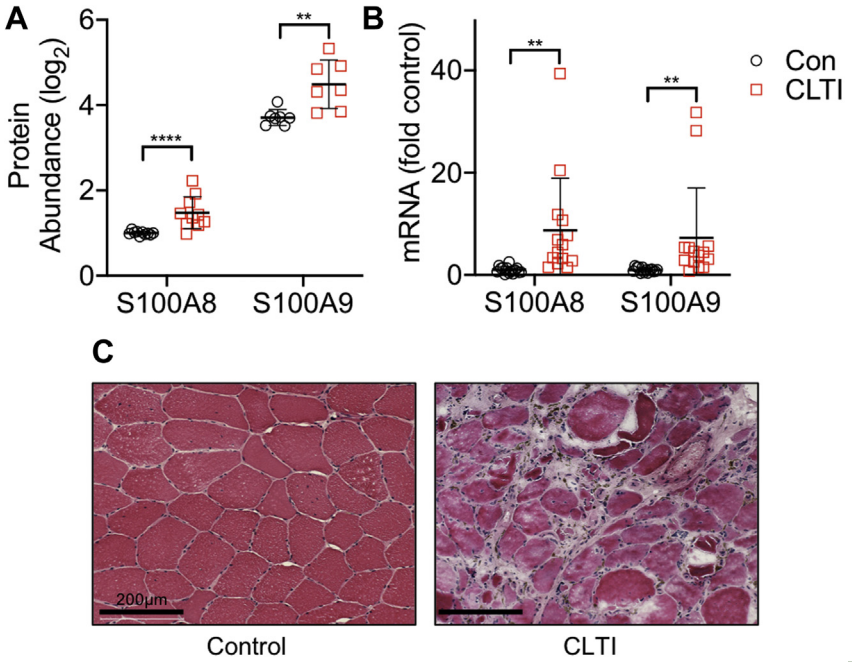

Fig 1. S100A8 and S100A9 (S100A8/A9) levels were elevated in chronic limb threatening ischemia (CLTI) limb muscle. **A,** Proteomic analysis of non–peripheral arterial disease (PAD) control (*Con*) and CLTI limb muscle with protein abundance converted to the Log2 space (n = 7-10/group). **B,** mRNA levels of S100A8/A9 were also elevated in limb muscle specimens compared with the Con group (n = 14/group). **C,** Representative hematoxylin and eosin–stained transverse sections of the gastrocnemius muscle from Con and CLTI participants. $^{**}P < .01$ and $^{****}P < .0001$ using two-tailed *t* test.

Treatment with S100A8/A9 impairs muscle mitochondrial function in C57BL6J mice. Because the abundance of S100A8 and S100A9 in CLTI patient muscles was associated with the magnitude of mitochondrial impairment, we used this mitochondrial assay to determine whether treatment with rS100A8/A9 impaired mitochondrial function in mice. We found that mice treated with rS100A8/A9 displayed reduced mitochondrial oxygen consumption (JO_2) across a range of energy demands in both nonischemic (Fig 5, *A*) and ischemic (Fig 5, *B*) gastrocnemius muscle mitochondria. However, in contrast to the strong association between the abundance of S100A8/A9 and mitochondrial H_2O_2 production in CLTI muscles, mice treated with rS100A8/A9 did not display greater production rates of H_2O_2 in either limb (Fig 5, *C* and *D*).

Treatment with S100A8/A9 causes atrophy and mitochondrial impairment in cultured myotubes. To isolate the effects of rS100A8/A9 from the effects of impaired muscle perfusion (Fig 4, *B*) observed in the mouse experiment, we used a cultured myotube system in which matured myotubes were treated with rS100A8/A9 in normoxic culture conditions. C2C12 myotubes (day 7 of differentiation) were treated with 1000 ng/mL of rS100A8/A9 by supplementing the culture medium for 24 hours. rS100A8/A9 treatment resulted in significant myotube atrophy (Fig 6, *A* and *B*) compared with vehicle treated (PBS plus 0.1% BSA) myotubes. Next, we used the same physiologic mitochondrial phenotyping system to analyze a range of steady state energy demands (Fig 6, *C*). These analyses of mitochondrial oxidative phosphorylation confirmed that rS100A8/A9 treatment impaired mitochondrial oxidative phosphorylation (Fig 6, *D*) but did not alter mitochondrial H_2O_2 production (Fig 6, *E*). These findings were consistent with the observed changes in the mice treated with rS100A8/A9 and confirmed that these alarmins induce mitochondrial impairment in muscle cells.

DISCUSSION

Inflammation is common in patients with PAD and has been shown to be intimately linked to both the development and the progression of the disease.[1,4,5,40–43] PAD risk factors, including tobacco smoking and diabetes, both independently increase inflammation.[44] Previous studies have identified several inflammatory molecules, including C-reactive protein, interleukin-6, and soluble intracellular adhesion molecule-1, that have been linked with both the development of PAD and its associated health outcomes.[4,5,45–47] Although inflammation has generally been regarded as a contributing factor to the pathobiology of cardiovascular disease, including PAD, a recent study failed to replicate the prognostic abilities of C-reactive protein in patients with PAD.[48] Thus,

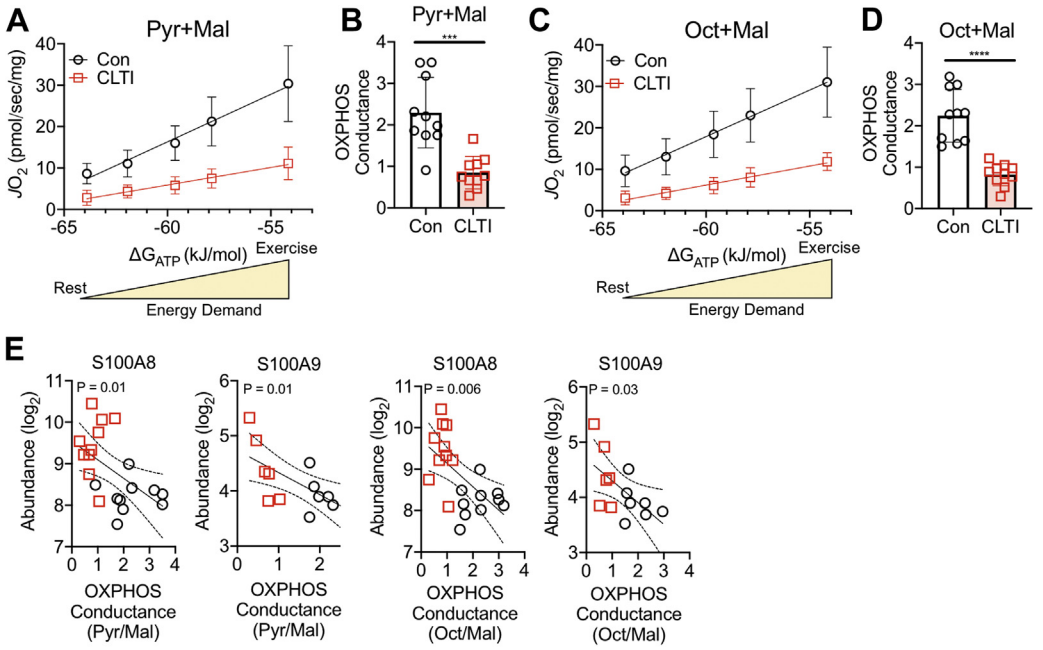

Fig 2. Mitochondrial deficits in chronic limb threatening ischemia (CLTI) were associated with S100A8 and S100A9 levels. Mitochondrial respiratory function was assessed using permeabilized muscle fibers exposed to a creatine kinase (CK) energetic clamp system to control the extra-mitochondrial adenosine diphosphate/adenosine triphosphate ratio, mimicking a stress test. **A,** Mitochondrial oxygen consumption (JO_2) across a range of steady state cellular energy demand (ΔG_{ATP}) levels supported by carbohydrates (pyruvate [*Pyr*] + malate [*Mal*]) demonstrated lower JO_2 in CLTI muscle compared with non–peripheral arterial disease (PAD) control (*Con*). **B,** Quantification of the slope in **A** provided an index of oxidative phosphorylation (*OXPHOS*) conductance (n = 10/group). **C,** Mitochondrial JO_2 across a range of steady state ΔG_{ATP} levels supported by fatty acids (octanoylcarnitine [*Oct*] + Mal) demonstrated lower JO_2 in CLTI muscle compared with non-PAD Con group. **D,** Quantification of the slope in **A** provides an index of OXPHOS conductance (n = 10/group). **E,** Pearson correlation demonstrated relationships between the protein abundance of S100A8/A9 and OXPHOS conductance with both carbohydrates and fatty acids. ***$P < .001$ and ****$P < .0001$, two-tailed *t* test.

much remains to be discovered regarding how inflammatory mediators affect PAD pathobiology.

Careful examination of a recently curated proteomics dataset from CLTI limb muscle indicated that S100A8/A9 proteins were significantly elevated in CLTI muscle compared with non-PAD control participants (Fig 1, *A*).[25] This finding was confirmed using mRNA analysis (Fig 1, *B*). S100A8/A9 are calcium binding proteins that belong to the S100 family. They are often found as heterodimers owing to the increased structural stability compared with homodimers. They are constitutively expressed in immune cells such as neutrophils and monocytes but will be released by these cells during inflammatory states.[6,49] The observation that S100A8/A9 abundance was elevated in the CLTI limb peaked our interest because recent studies had demonstrated that these calcium binding proteins might play a causal role in pathology after myocardial infarction.[9] S100A8/A9 protein levels increased with myocardial ischemia and were detectable in serum before other biochemical indicators of myocardial necrosis.[7,11] In a rodent model of postischemic heart failure, a study reported that S100A8/A9 mRNA and proteins levels increased rapidly following induction of ischemia and that treatment with recombinant S100A8/A9 impaired cardiac performance after ischemia and reperfusion.[10] Preclinical studies have shown that blockage of S100A8/A9 can improve cardiac pathology after myocardial ischemia.[19,49]

Mechanistically, a recent study indicated that S100A8/A9 proteins are linked to myocardial ischemic pathology via inhibition of mitochondrial metabolism in cardiomyocytes.[18] Our group, and others, reported that aberrant mitochondrial metabolism is a common feature of limb muscle specimens from PAD/CLTI patients.[24,50–55] Using permeabilized muscle fibers and high respirometry, such as in our previous study,[24] we assessed muscle mitochondrial metabolism using a novel energy clamp system that assesses mitochondrial oxygen consumption across a range of physiologic energy demands (similar to a stress test).[28–30] Consistent with previous findings, CLTI muscle displayed a significant impairment in mitochondrial oxidative phosphorylation (Fig 2, *A-D*). The degree of mitochondrial impairment correlated strongly with the S100A8 and S100A9 protein levels (Fig 2, *E*).

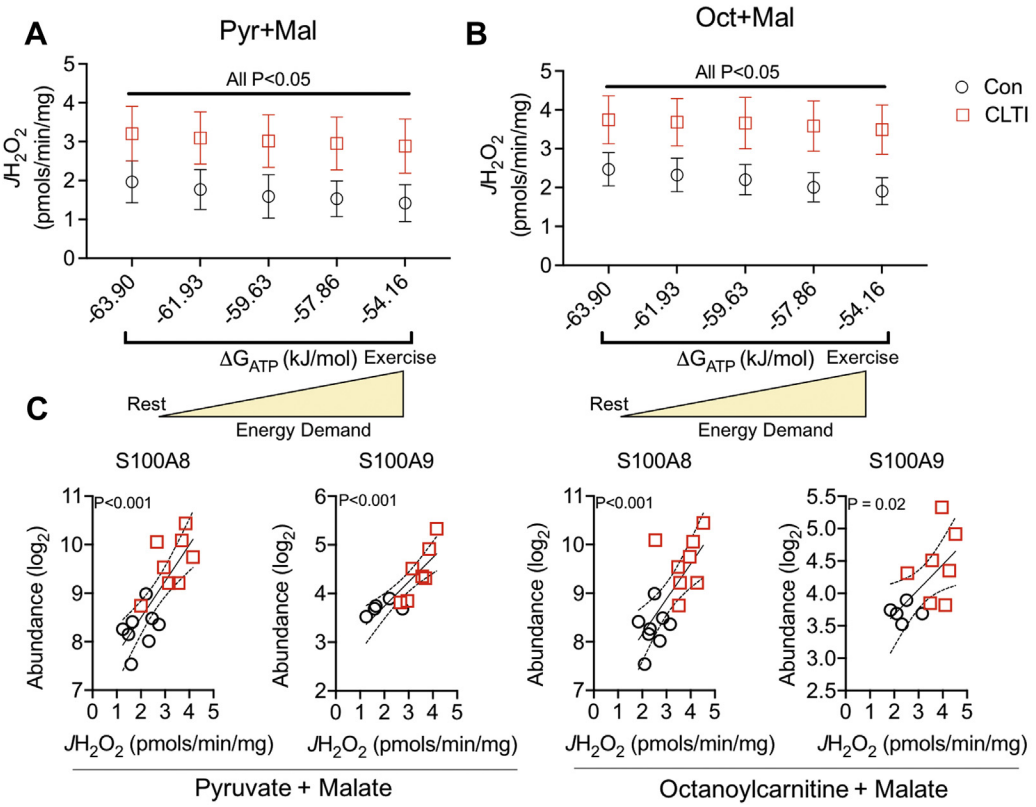

Fig 3. Mitochondrial hydrogen peroxide (H_2O_2) production was higher in chronic limb threatening ischemia (CLTI) and was associated with higher S100A8/A9 levels. Mitochondrial H_2O_2 production was assessed using permeabilized muscle fibers exposed to a creatine kinase (CK) energetic clamp system to control the extramitochondrial adenosine diphosphate/adenosine triphosphate ratio, mimicking a stress test. Supported by carbohydrates (pyruvate [*Pyr*] + malate [*Mal*]; **A**) or fatty acids (octanoylcarnitine [*Oct*] + Mal; **B**), CLTI muscle fibers had greater rates of mitochondrial H_2O_2 production than did the non-PAD control (*Con*) across the entire range of energy demands tested (n = 10/group). **C,** Rates of H_2O_2 production at an energy demand similar to that of resting muscle (cellular energy demand [ΔG_{ATP}], −63.90 kJ/mol) correlated strongly with the abundance of S100A8 and S100A9 proteins.

Mitochondrial H_2O_2 production was also greater in the CLTI muscle than in the non-PAD control muscle (Fig 3, *A* and *B*). Also, the level of H_2O_2 production at a resting level of energy demand correlated with the S100A8/A9 protein levels (Fig 3, *C*).

To determine whether elevated S100A8/A9 levels could regulate ischemic limb pathology, we used the established hindlimb ischemia model in C57BL6 mice—a genetic strain known to be relatively resistant to CLTI symptoms.[31,33,37,38,56–58] Consistent with worsening ischemic myocardial function,[10] the mice given intraperitoneal injections of recombinant S100A8/A9 displayed impaired perfusion recovery after induction of hindlimb ischemia (Fig 4, *B*). Our finding of impaired limb perfusion recovery in the S100A8/A9-treated mice subjected to hindlimb ischemia was supported in part by a previous study. Ganta et al[22] reported that the antiangiogenic isoform $VEGF_{165}b$, which is elevated in PAD limb muscle, inhibits VEGFR1 in macrophages, causing the S100A8/A9-mediated M1-like phenotype and impairing angiogenesis and perfusion recovery in ischemic muscle. The findings from the present study have extended the increasing body of literature demonstrating that macrophage maturation plays a critical role in arteriogenesis and angiogenesis—a process highly relevant to the CLTI population.[59–61] These findings have shown that it is plausible that the injected rS100A8/A9 could have negatively affected macrophages, contributing to the observed impairment in perfusion recovery (Fig 3, *B*), although flow cytometry-based assessments of macrophage maturation and polarization were not performed in the present study.

Given the striking correlation between the abundance of S100A8/A9 and mitochondrial impairment in CLTI patient muscle specimens, we also assessed the limb muscle mitochondrial function in mice treated with either placebo or rS100A8/A9. Consistent with the findings in cardiomyocytes, the mice treated with rS100A8/A9 exhibited impairments in muscle mitochondrial oxidative phosphorylation in both nonischemic and ischemic

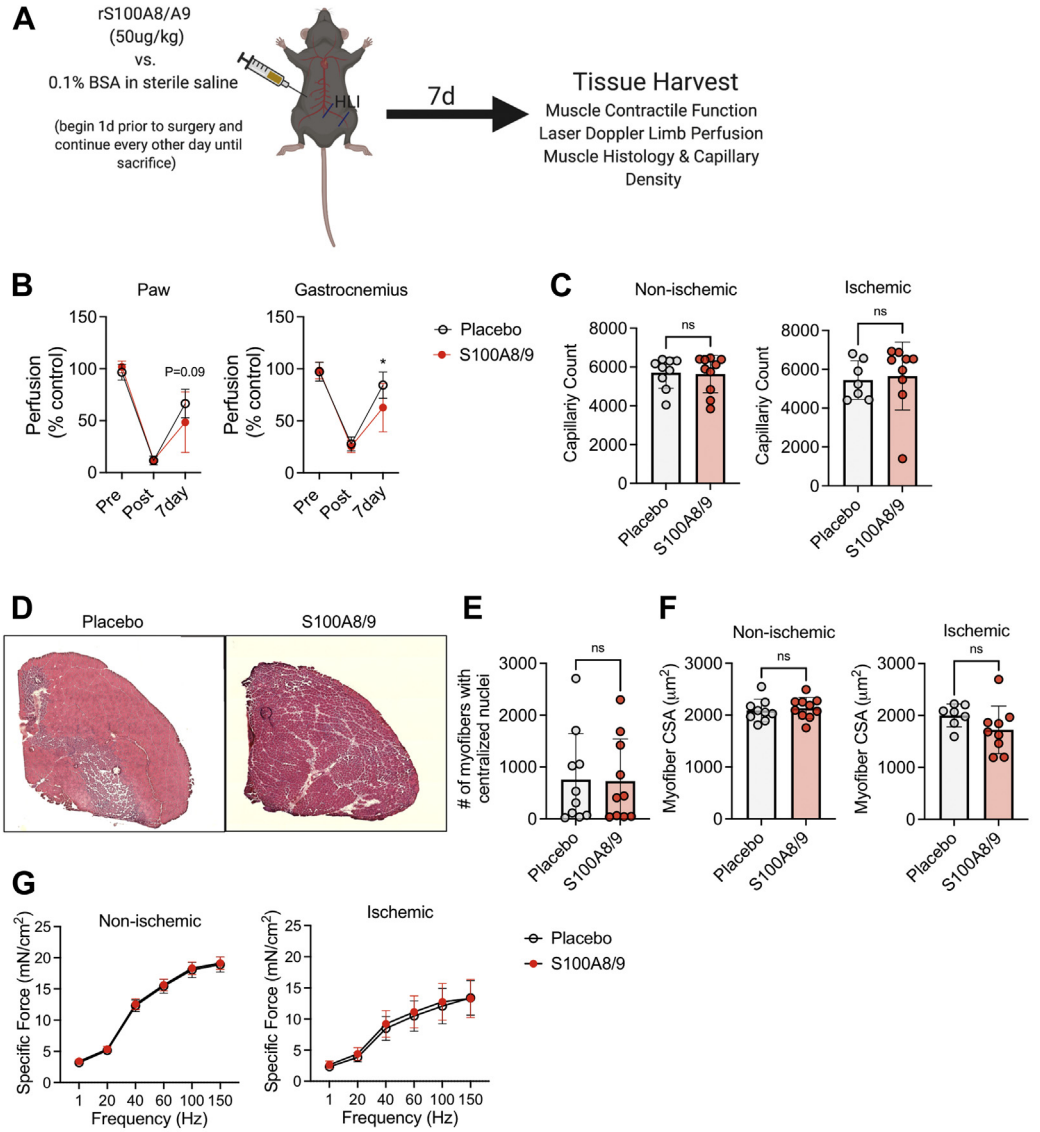

Fig 4. Treatment with recombinant S100A8 and S100A9 (rS100A8/A9) impaired limb perfusion recovery but not muscle force production in mice subjected to hindlimb ischemia. **A,** Schematic of the mouse model of hindlimb ischemia with either placebo or rS100A8/A9 treatment. **B,** Laser Doppler perfusion recovery in the paw and gastrocnemius muscle. **C,** Capillary density in the tibialis anterior muscle of the nonischemic and ischemic limb of mice. **D,** Representative hematoxylin and eosin–stained tibialis anterior muscles indicating mild injury. **E,** Quantification of the number of myofibers with centralized nuclei (indicating muscle injury and/or regeneration). **F,** Quantification of the myofiber cross-sectional area in the nonischemic and ischemic tibialis anterior muscles. **G,** Muscle force production measured ex vivo in the extensor digitorum longus muscles (n = 10/group). *$P < .05$, repeated measures analysis of variance.

gastrocnemius muscles (Fig 5, *A* and *B*).[18] This finding of S100A8/A9-mediated mitochondrial respiratory impairment was also confirmed in a cultured myotube system in which oxygen availability was not limiting (Fig 6). Taken together, these findings have confirmed that, similar to cardiomyocytes, S100A8/A9 can directly impair skeletal muscle mitochondrial function.[18] Although rS100A8/A9 treatment in mice impaired mitochondrial respiration, it did not increase mitochondrial H_2O_2 production (Fig 5). The rate of H_2O_2 production in these experiments was dependent on the balance between the rate of production and the rate of scavenging by the numerous antioxidant systems resident in mitochondria. Thus, a decrease in the rate of respiration is not a direct predictor of H_2O_2 or superoxide production.[62] Moreover, it is important to recognize that within the assay conditions used, mitochondria were exposed to physiologically relevant energy demands in which very few electrons flowing through the electron transport system will leak prematurely to or from superoxide or H_2O_2.[62,63]

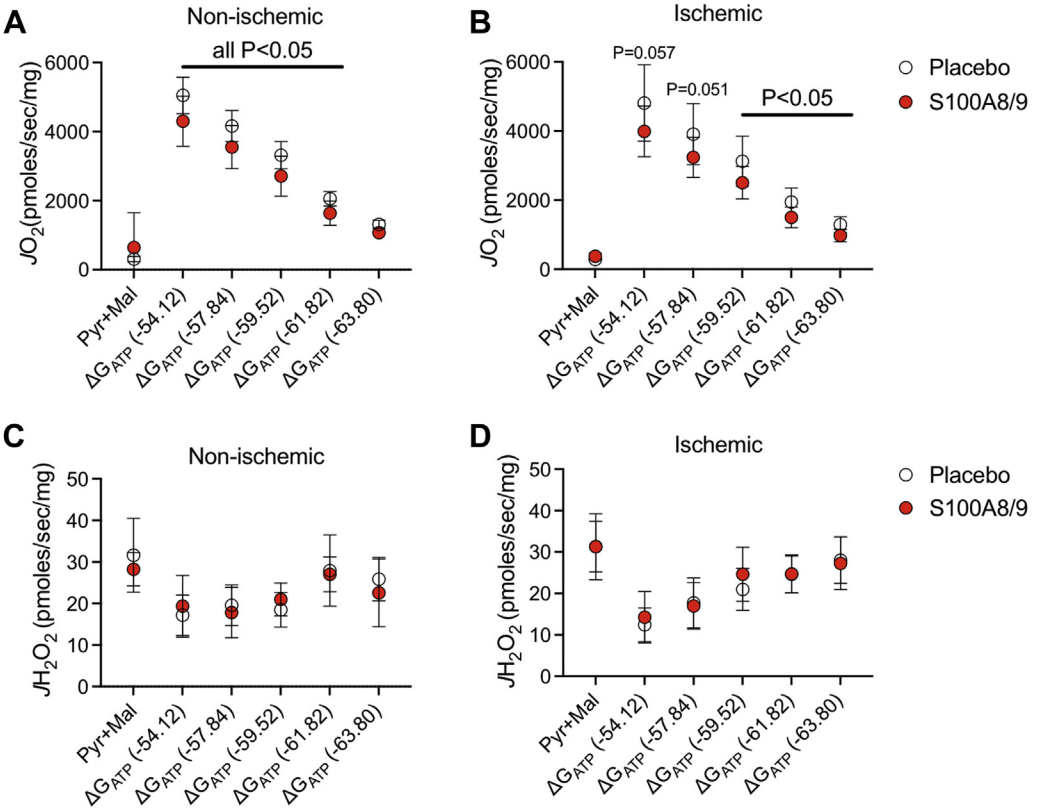

Fig 5. Treatment with recombinant S100A8 and S100A9 (rS100A8/A9) induced mild mitochondrial impairment in nonischemic and ischemic muscle. **A,** Mitochondrial respiratory function across a range of physiologic energy demands was lower in the nonischemic muscle of mice treated with rS100A8/A9. **B,** Mitochondrial respiratory function across a range of physiologic energy demands was lower in the ischemic muscle of mice treated with rS100A8/A9. Mitochondrial hydrogen peroxide (H_2O_2) production was not different between the placebo- and rS100A8/A9-treated mice in nonischemic (**C**) or ischemic (**D**) gastrocnemius muscle (n = 10/group). Statistical analysis was performed using a two-tailed *t* test.

Despite decreasing limb perfusion recovery and mitochondrial respiration, treatment with S100A8/A9 did not alter the muscle capillary content or muscle contractile force, assessed ex vivo in an isolated organ bath. A possible explanation for these observations might be related to the magnitude of mitochondrial impairment. Treatment with S100A8/A9 at 50 μg/kg body weight produced a modest (~10%) reduction in mitochondrial respiration at higher energy demands. The magnitude of difference in mitochondrial respiration between the placebo- and rS100A8/A9-treated mice at lower levels of energy demand (eg, ΔG_{ATP}, 63.8 kJ/mol) was much <10% (Fig 5). Therefore, future studies are warranted to explore the dose-dependent effects of S100A8/A9 in ischemic limb pathology.

The present study had several limitations that warrant discussion. First, the analyses involving CLTI patients should be considered preliminary because the sample size was limited and the patient phenotyping was not sufficiently detailed. Future cohort studies with larger patient numbers are required to examine the link between the serum and muscle levels of S100A8/A9 and CLTI disease severity. Additionally, the percentage of female participants in the present study was low; however, CLTI is prevalent in both male and female older adults. Second, although the proteomics analysis was considered robust, the limited specimen size for the non-PAD controls precluded our ability to validate protein levels using a different technique. However, we were able to confirm that the mRNA levels of S100A8/A9 were elevated, consistent with the proteomic results. Third, we did not perform analyses to determine the degree of systemic inflammation in the participants in the present study. Considering that S100A8/A9 levels are increased during states of inflammation, these analyses would be important to consider for both non-PAD and CLTI patients and could affect the interpretation of our preliminary clinical data. Fourth, the preclinical model we used was of C57BL6J mice, which are known to be resistant to limb ischemia and not adequately representative of CLTI.[31,33,37,38,58] The C57BL6J strain was chosen because ischemia-sensitive strains, such as BALB/c, display severe

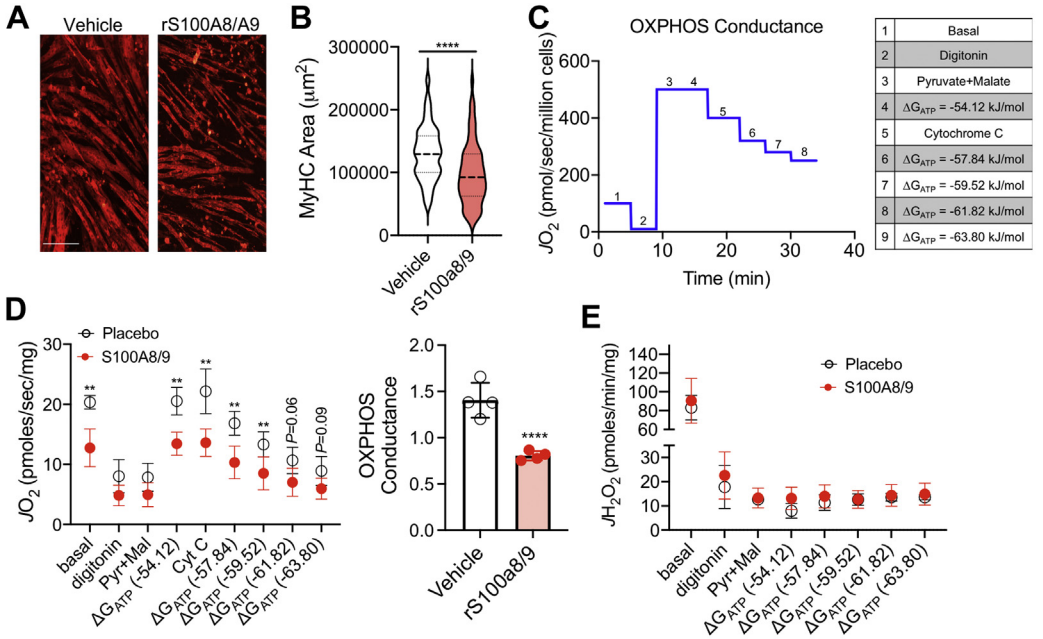

Fig 6. Treatment with recombinant S100A8 and S100A9 (rS100A8/A9) caused atrophy and mitochondrial respiratory impairment in cultured myotubes. **A,** Representative images (stained for myosin) of cultured C2C12 myotubes treated with vehicle (phosphate-buffered saline [PBS] plus 0.1% bovine serum albumin [BSA]) or rS100A8/A9 (1000 ng/mL) for 24 hours (scale bar = 150 μm). **B,** Quantification of the myotube area (stained for myosin heavy chain) demonstrated atrophy after treatment with rS100A8/A9. **C,** Schematic showing the mitochondrial protocol used in these myotubes. **D,** Mitochondrial oxidative phosphorylation was impaired in myotubes treated with rS100A8/A9. **E,** Mitochondrial hydrogen peroxide (H_2O_2) production was not altered by rS100A8/A9 treatment in myotubes (n = 4 biologically independent samples/group). $^{**}P < .01$ and $^{****}P < .0001$, two-tailed *t* test.

ischemic muscle mitochondrial pathology after induction of hindlimb ischemia, such that detecting exacerbation of the pathology with exogenous S100A8/A9 treatment could have proved difficult.[38] Furthermore, mice used in the present study were male only, young in age, and free of comorbid diseases such as diabetes, hypertension, hyperlipidemia, obesity, and renal disease, all of which are likely to increase the likelihood of systemic inflammation. Thus, they do not model the CLTI patient characteristics well. Another consideration is that samples from the CLTI patients were obtained from the gastrocnemius muscle. However, in our mouse experiment, it was not possible to perform all the analyses using the gastrocnemius muscle because this entire muscle was needed for the mitochondrial isolation procedures, and other functional measures were not possible using this same muscle.

CONCLUSIONS

In the present study, we found that the S100A8 and S100A9 protein levels were elevated in the limb muscle of CLTI patients and that these levels were strongly associated with the degree of mitochondrial impairment. The treatment of mice with rS100A8/A9 impaired limb perfusion recovery and mitochondrial function after hindlimb ischemia. These findings highlight the possible role of S100A8/A9 in ischemic limb pathology and indicate that future studies examining the therapeutic potential of pharmacologic blockades of these inflammatory mediators are warranted.

AUTHOR CONTRIBUTIONS

Conception and design: ZS, TR
Analysis and interpretation: ZS, VM, NB, RK, NV, TT, KV, SB, SS, GV, TR
Data collection: ZS, VM, NB, RK, NV, TT, KV, SB, SS, GV, TR
Writing the article: ZS, TR
Critical revision of the article: ZS, VM, NB, RK, NV, TT, KV, SB, SS, GV, TR
Final approval of the article: ZS, VM, NB, RK, NV, TT, KV, SB, SS, GV, TR
Statistical analysis: ZS, TR
Obtained funding: TR
Overall responsibility: TR

REFERENCES

1. Ding N, Yang C, Ballew SH, Kalbaugh CA, McEvoy JW, Salameh M, et al. Fibrosis and inflammatory markers and long-term risk of peripheral artery disease: the ARIC study. Arterioscler Thromb Vasc Biol 2020;40:2322-31.

2. Casale GP, Thompson JR, Carpenter LC, Kim J, Lackner TJ, Mietus CJ, et al. Cytokine signature of inflammation mediated by autoreactive Th-cells, in calf muscle of claudicating patients with Fontaine stage II peripheral artery disease. Transl Res 2021;228:94-108.
3. Erdogan SB, Selcuk UN, Bastopcu M, Arslanhan G, Cakmak AY, Kuplay H, et al. Critical limb ischemia patients clinically improving with medical treatment have lower neutrophil-to-lymphocyte and platelet-to-lymphocyte ratios. Vascular 2021;29:920-6.
4. Tzoulaki I, Murray GD, Lee AJ, Rumley A, Lowe GDO, Fowkes FGR. Inflammatory, haemostatic, and rheological markers for incident peripheral arterial disease: edinburgh artery study. Eur Heart J 2007;28:354-62.
5. Ridker PM, Stampfer MJ, Rifai N. Novel risk factors for systemic atherosclerosis—a comparison of C-reactive protein, fibrinogen, homocysteine, lipoprotein(a), and standard cholesterol screening as predictors of peripheral arterial disease. JAMA 2001;285:2481-5.
6. Boyd JH, Kan B, Roberts H, Wang YJ, Walley KR. S100A8 and S100A9 mediate endotoxin-induced cardiomyocyte dysfunction via the receptor for advanced glycation end products. Circ Res 2008;102:1239-46.
7. Katashima T, Naruko T, Terasaki F, Fujita M, Otsuka K, Murakami S, et al. Enhanced expression of the S100A8/A9 complex in acute myocardial infarction patients. Circ J 2010;74:741-8.
8. Dragu A, Schnurer S, Surmann-Schmitt C, von der Mark K, Sturzl M, Unglaub F, et al. Gene expression analysis of ischaemia and reperfusion in human microsurgical free muscle tissue transfer. J Cel Mol Med 2011;15:983-93.
9. Frangogiannis NG. S100A8/A9 as a therapeutic target in myocardial infarction: cellular mechanisms, molecular interactions, and translational challenges. Eur Heart J 2019;40:2724-6.
10. Volz HC, Laohachewin D, Seidel C, Lasitschka F, Keilbach K, Wienbrandt AR, et al. S100A8/A9 aggravates post-ischemic heart failure through activation of RAGE-dependent NF-kappa B signaling. Basic Res Cardiol 2012;107:250.
11. Altwegg LA, Neidhart M, Hersberger M, Muller S, Eberli FR, Corti R, et al. FASTTRACK—myeloid-related protein 8/14 complex is released by monocytes and granulocytes at the site of coronary occlusion: a novel, early, and sensitive marker of acute coronary syndromes. Eur Heart J 2007;28:941-8.
12. Sreejit G, Flynn MC, Patil M, Krishnamurthy P, Murphy AJ, Nagareddy PR. S100 family proteins in inflammation and beyond. Adv Clin Chem 2020;98:173-231.
13. Sreejit G, Latif AA, Murphy AJ, Nagareddy PR. Emerging roles of neutrophil-borne S100A8/A9 in cardiovascular inflammation. Pharmacol Res 2020;161:105212.
14. Wang SW, Song R, Wang ZY, Jing ZC, Wang SX, Ma J. S100A8/A9 in inflammation. Front Immunol 2018;9:1298.
15. Hofmann MA, Drury S, Fu CF, Qu W, Taguchi A, Lu Y, et al. RAGE mediates a novel proinflammatory axis: a central cell surface receptor for S100/calgranulin polypeptides. Cell 1999;97:889-901.
16. Ehrchen JM, Sunderkotter C, Foell D, Vogl T, Roth J. The endogenous toll-like receptor 4 agonist S100A8/S100A9 (calprotectin) as innate amplifier of infection, autoimmunity, and cancer. J Leukoc Biol 2009;86:557-66.
17. Cotoi OS, Duner P, Ko N, Hedblad B, Nilsson J, Bjorkbacka H, et al. Plasma S100A8/A9 correlates with blood neutrophil counts, traditional risk factors, and cardiovascular disease in middle-aged healthy individuals. Arterioscler Thromb Vasc Biol 2014;34:202-10.
18. Li YL, Chen BY, Yang XY, Zhang CC, Jiao Y, Li P, et al. S100a8/a9 signaling causes mitochondrial dysfunction and cardiomyocyte death in response to ischemic/reperfusion injury. Circulation 2019;140:751-64.
19. Marinkovic G, Larsen HG, Yndigegn T, Szabo IA, Mares RG, de Camp L, et al. Inhibition of pro-inflammatory myeloid cell responses by short-term S100A9 blockade improves cardiac function after myocardial infarction. Eur Heart J 2019;40:2713-23.
20. Saenz-Pipaon G, San Martin P, Planell N, Maillo A, Ravassa S, Vilas-Zornoza A, et al. Functional and transcriptomic analysis of extracellular vesicles identifies calprotectin as a new prognostic marker in peripheral arterial disease (PAD). J Extracell Vesicles 2020;9:1729646.
21. Kraakman MJ, Lee MKS, Al-Sharea A, Dragoljevic D, Barrett TJ, Montenont E, et al. Neutrophil-derived S100 calcium-binding proteins A8/A9 promote reticulated thrombocytosis and atherogenesis in diabetes. J Clin Invest 2017;127:2133-47.
22. Ganta VC, Choi M, Farber CR, Annex BH. Antiangiogenic VEGF(165)b regulates macrophage polarization via S100A8/S100A9 in peripheral artery disease. Circulation 2019;139:226-42.
23. Ryan TE, Brophy P, Lin CT, Hickner RC, Neufer PD. Assessment of in vivo skeletal muscle mitochondrial respiratory capacity in humans by near-infrared spectroscopy: a comparison with in situ measurements. J Physiol 2014;592:3231-41.
24. Ryan TE, Yamaguchi DJ, Schmidt CA, Zeczycki TN, Shaikh SR, Brophy P, et al. Extensive skeletal muscle cell mitochondriopathy distinguishes critical limb ischemia patients from claudicants. JCI Insight 2018;3:e123235.
25. Ryan TE, Kim K, Scali ST, Berceli SA, Thome T, Salyers ZR, et al. Interventional- and amputation-stage muscle proteomes in the chronically threatened ischemic limb. Clin Transl Med 2022;12:e658.
26. Perry CG, Kane DA, Lin CT, Kozy R, Cathey BL, Lark DS, et al. Inhibiting myosin-ATPase reveals a dynamic range of mitochondrial respiratory control in skeletal muscle. Biochem J 2011;437:215-22.
27. Fisher-Wellman KH, Lin CT, Ryan TE, Reese LR, Gilliam LA, Cathey BL, et al. Pyruvate dehydrogenase complex and nicotinamide nucleotide transhydrogenase constitute an energy-consuming redox circuit. Biochem J 2015;467:271-80.
28. Thome T, Salyers ZR, Kumar RA, Hahn D, Berru FN, Ferreira LF, et al. Uremic metabolites impair skeletal muscle mitochondrial energetics through disruption of the electron transport system and matrix dehydrogenase activity. Am J Physiol Cel Physiol 2019;317:C701-13.
29. Fisher-Wellman KH, Davidson MT, Narowski TM, Lin CT, Koves TR, Muoio DM. Mitochondrial diagnostics: a multiplexed assay platform for comprehensive assessment of mitochondrial energy fluxes. Cell Rep 2018;24:3593-3606.e10.
30. Thome T, Kumar RA, Burke SK, Khattri RB, Salyers ZR, Kelley RC, et al. Impaired muscle mitochondrial energetics is associated with uremic metabolite accumulation in chronic kidney disease. JCI Insight 2021;6:e139826.
31. Dokun AO, Keum S, Hazarika S, Li Y, Lamonte GM, Wheeler F, et al. A quantitative trait locus (LSq-1) on mouse chromosome 7 is linked to the absence of tissue loss after surgical hindlimb ischemia. Circulation 2008;117:1207-15.
32. Ryan TE, Schmidt CA, Green TD, Spangenburg EE, Neufer PD, McClung JM. Targeted expression of catalase to mitochondria protects against ischemic myopathy in high-fat diet-fed mice. Diabetes 2016;65:2553-68.
33. McClung JM, McCord TJ, Ryan TE, Schmidt CA, Green TD, Southerland KW, et al. BAG3 (Bcl-2-associated athanogene-3) coding variant in mice determines susceptibility to ischemic limb muscle myopathy by directing autophagy. Circulation 2017;136:281-96.
34. Ryan TE, Schmidt CA, Green TD, Spangenburg EE, Neufer PD, McClung JM. Targeted expression of catalase to mitochondria protects against ischemic myopathy in high fat fed mice. Diabetes 2016;65:2553-68.
35. Berru FN, Gray SE, Thome T, Kumar RA, Salyers ZR, Coleman M, et al. Chronic kidney disease exacerbates ischemic limb myopathy in mice via altered mitochondrial energetics. Sci Rep 2019;9:15547.
36. Mayeuf-Louchart A, Hardy D, Thorel Q, Roux P, Gueniot L, Briand D, et al. MuscleJ: a high-content analysis method to study skeletal muscle with a new Fiji tool. Skelet Muscle 2018;8:25.
37. Schmidt CA, Ryan TE, Lin CT, Inigo MMR, Green TD, Brault JJ, et al. Diminished force production and mitochondrial respiratory deficits are strain-dependent myopathies of subacute limb ischemia. J Vasc Surg 2017;65:1504-14.e11.
38. Ryan TE, Schmidt CA, Tarpey MD, Amorese AJ, Yamaguchi DJ, Goldberg EJ, et al. PFKFB3-mediated glycolysis rescues myopathic outcomes in the ischemic limb. JCI Insight 2020;5:e139628.
39. Mendez J, Keys A. Density and composition of mammalian muscle. Metabolism 1960;9:184-8.
40. McDermott MM, Guralnik JM, Corsi A, Albay M, Macchi C, Bandinelli S, et al. Patterns of inflammation associated with peripheral arterial disease: the InCHIANTI study. Am Heart J 2005;150:276-81.
41. Brevetti G, Piscione F, Cirillo P, Galasso G, Schiano V, Barbato E, et al. In concomitant coronary and peripheral arterial disease, inflammation of the affected limbs predicts coronary artery endothelial dysfunction. Atherosclerosis 2008;201:440-6.
42. Gardner AW, Parker DE, Montgomery PS, Sosnowska D, Casanegra AI, Ungvari Z, et al. Endothelial cell inflammation and antioxidant capacity are associated with exercise performance and

microcirculation in patients with peripheral artery disease. Circulation 2014;130:A12280.
43. Rein P, Saely CH, Silbernagel G, Vonbank A, Mathies R, Drexel H, et al. Systemic inflammation is higher in peripheral artery disease than in stable coronary artery disease. Atherosclerosis 2015;239:299-303.
44. Fowkes FGR, Housley E, Riemersma RA, Macintyre CCA, Cawood EHH, Prescott RJ, et al. Smoking, lipids, glucose intolerance, and blood pressure as risk factors for peripheral atherosclerosis compared with ischemic heart disease in the Edinburgh artery study. Am J Epidemiol 1992;135:331-40.
45. Brevetti G, Giugliano G, Brevetti L, Hiatt WR. Inflammation in peripheral artery disease. Circulation 2010;122:1862-75.
46. Ridker PM, Cushman M, Stampfer MJ, Tracy RP, Hennekens CH. Plasma concentration of C-reactive protein and risk of developing peripheral vascular disease. Circulation 1998;97:425-8.
47. Rossi E, Biasucci LM, Citterio F, Pelliccioni S, Monaco C, Ginnetti F, et al. Risk of myocardial infarction and angina in patients with severe peripheral vascular disease—predictive role of C-reactive protein. Circulation 2002;105:800-3.
48. Brevetti G, Schiano V, Laurenzano E, Giugliano G, Petretta M, Scopacasa F, et al. Myeloperoxidase, but not C-reactive protein, predicts cardiovascular risk in peripheral arterial disease. Eur Heart J 2008;29:224-30.
49. Sreejit G, Abdel-Latif A, Athmanathan B, Annabathula R, Dhyani A, Noothi SK, et al. Neutrophil-derived S100A8/A9 amplify granulopoiesis after myocardial infarction. Circulation 2020;141:1080-94.
50. Pipinos II, Sharov VG, Shepard AD, Anagnostopoulos PV, Katsamouris A, Todor A, et al. Abnormal mitochondrial respiration in skeletal muscle in patients with peripheral arterial disease. J Vasc Surg 2003;38:827-32.
51. Pipinos II, Judge AR, Zhu Z, Selsby JT, Swanson SA, Johanning JM, et al. Mitochondrial defects and oxidative damage in patients with peripheral arterial disease. Free Radic Biol Med 2006;41:262-9.
52. Pizzimenti M, Riou M, Charles AL, Talha S, Meyer A, Andres E, et al. The rise of mitochondria in peripheral arterial disease physiopathology: experimental and clinical data. J Clin Med 2019;8:2125.
53. Gonzalez-Freire M, Moore AZ, Peterson CA, Kosmac K, McDermott MM, Sufit RL, et al. Associations of peripheral artery disease with calf skeletal muscle mitochondrial DNA heteroplasmy. J Am Heart Assoc 2020;9:e015197.
54. Groennebaek T, Billeskov TB, Schytz CT, Jespersen NR, Botker HE, Olsen RKJ, et al. Mitochondrial structure and function in the metabolic myopathy accompanying patients with critical limb ischemia. Cells 2020;9:570.
55. Khattri RB, Kim K, Thome T, Salyers ZR, O'Malley KA, Berceli SA, et al. Unique metabolomic profile of skeletal muscle in chronic limb threatening ischemia. J Clin Med 2021;10:548.
56. McClung JM, McCord TJ, Keum S, Johnson S, Annex BH, Marchuk DA, et al. Skeletal muscle-specific genetic determinants contribute to the differential strain-dependent effects of hindlimb ischemia in mice. Am J Pathol 2012;180:2156-69.
57. McClung JM, McCord TJ, Southerland K, Schmidt CA, Padgett ME, Ryan TE, et al. Subacute limb ischemia induces skeletal muscle injury in genetically susceptible mice independent of vascular density. J Vasc Surg 2016;64:1101-11.e2.
58. Schmidt CA, Amorese AJ, Ryan TE, Goldberg EJ, Tarpey MD, Green TD, et al. Strain-dependent variation in acute ischemic muscle injury. Am J Pathol 2018;188:1246-62.
59. Krishnasamy K, Limbourg A, Kapanadze T, Gamrekelashvili J, Beger C, Hager C, et al. Blood vessel control of macrophage maturation promotes arteriogenesis in ischemia. Nat Commun 2017;8:952.
60. Ganta VC, Choi MH, Kutateladze A, Fox TE, Farber CR, Annex BH. A microRNA93-interferon regulatory factor-9-immunoresponsive gene-1-itaconic acid pathway modulates M2-like macrophage polarization to revascularize ischemic muscle. Circulation 2017;135:2403-24.
61. Patel AS, Smith A, Nucera S, Biziato D, Saha P, Attia RQ, et al. TIE2-expressing monocytes/macrophages regulate revascularization of the ischemic limb. EMBO Mol Med 2013;5:858-69.
62. Brand MD. Riding the tiger—physiological and pathological effects of superoxide and hydrogen peroxide generated in the mitochondrial matrix. Crit Rev Biochem Mol 2020;55:592-661.
63. Goncalves RLS, Quinlan CL, Perevoshchikova IV, Hey-Mogensen M, Brand MD. Sites of superoxide and hydrogen peroxide production by muscle mitochondria assessed ex vivo under conditions mimicking rest and exercise. J Biol Chem 2015;290:209-27.

Submitted Dec 15, 2021; accepted Mar 22, 2022.